BIOCHEMICAL PHARMACOLOGY 75 (2008) 360–368

available at www.sciencedirect.com

ScienceDirect

journal homepage: www.elsevier.com/locate/biochempharm

Anticancer mechanisms of YC-1 in human lung cancer cell line, NCI-H226

Chun-Jen Chen [a], *Mei-Hua Hsu* [a], *Li-Jiau Huang* [a], *Takao Yamori* [b], *Jing-Gung Chung* [c], *Fang-Yu Lee* [d], *Che-Ming Teng* [e], *Sheng-Chu Kuo* [a,*]

[a] *Graduate Institute of Pharmaceutical Chemistry, China Medical University, No. 91, Hsueh-Shih Road, Taichung 40421, Taiwan, ROC*
[b] *Division of Experimental Chemotherapy, Cancer Chemotherapy Cancer, Japanese Foundation for Cancer Research, Tokyo 170-8455, Japan*
[c] *Graduate Institute of Medical Science, China Medical University, Taichung, Taiwan, ROC*
[d] *Yung-Shin Pharmaceutical Industry Co., Ltd., Taichung, Taiwan, ROC*
[e] *Pharmacological Institute, College of Medicine, National Taiwan University, Taipei, Taiwan, ROC*

ARTICLE INFO

Article history:
Received 5 June 2007
Accepted 10 August 2007

Keywords:
YC-1
NCI-H226
Cell cycle arrest
Apoptosis
Anti-metastasis

ABSTRACT

As part of a continuing search for potential anticancer drug candidates, 1-benzyl-3-(5-hydroxymethyl-2-furyl)indazole (YC-1) was evaluated in the Japanese Cancer Institute's (JCI) *in vitro* disease-oriented anticancer screen. The results indicated that YC-1 showed impressive selective toxicity against the NCI-H226 cell line. Therefore, the molecular mechanism by which YC-1 affects NCI-H226 cell growth was studied. YC-1 inhibited NCI-H226 cell growth in a time- and a concentration-dependent manner. YC-1 suppressed the protein levels of cyclin D1, CDK2 and cdc25A, up-regulated p16, p21 and p53, increased the number of NCI-H226 cells in the G0/G1 phase of the cell cycle. Long exposure to YC-1 induced apoptosis by mitochondrial-dependent pathway. In addition, YC-1 inhibited MMP-2 and MMP-9 protein activities to abolish tumor cells metastasis. These findings suggest a mechanism of cytotoxic action of YC-1 and indicate that YC-1 may be a promising chemotherapy agent against lung cancer.

1. Introduction

Cancer can be regarded as a heterogeneous group of proliferative diseases, resulting from the accumulation of genetic lesions. Despite considerable advances in our understanding of the molecular mechanisms of carcinogenesis, cancer remains the first or second major cause of death due to medical causes in the United States as well as many of the developed world [1,2]. Thus there is an urgent need for new, efficacious and specific anticancer approaches. The identification of genetic alterations in cancer cells such as mutations in tumor oncogenes and tumor suppressor genes, the impaired ability of cancer cells to undergo apoptosis and the discovery of potent and specific, rationally designed drugs against molecular targets have developed into the era of targeted therapy [3].

In our previous works, we have synthesized a series of 1-arylmethyl-3-aryl-imidazole derivatives and found that

* *Corresponding author*. Tel.: +886 4 22030760; fax: +886 4 22030760.
E-mail address: sckuo@mail.cmu.edu.tw (S.-C. Kuo).

Abbreviations: bFGF, basic fibroblast growth factor; DMSO, dimethyl sulfoxide; ERK, extracellular signal-regulated kinase; FBS, fetal bovine serum; FACS, fluorescence-activated cell sorter; JNK, c-Jun NH_2-terminal kinase; MAPKs, mitogen-activated protein kinases; MMPs, matrix metalloproteinases; MTT, 3-(4,5-dimethylthiazol-2-yl)-2,5-diphenyltetrazolium bromide; PI, propidium iodide; sGC, soluble guanylate cyclase; SRB, sulforhodamine B; VEGF, vascular endothelial growth factor; YC-1, 1-benzyl-3-(5-hydroxymethyl-2-furyl)indazole.

0006-2952/$ – see front matter © 2007 Published by Elsevier Inc.
doi:10.1016/j.bcp.2007.08.011

1-benzyl-3-(5-hydroxymethyl-2-furyl)indazole (YC-1) was the most promising anti-platelet agent [4,5]. Subsequent investigation of its action mechanism demonstrated that YC-1 is a unique NO-independent, and NO-enhancing, activator of soluble guanylate cyclase (sGC) [6,7]. Because sGC is associated with many physiological functions, a lot of papers with the biological functions and pharmacological action of YC-1 have been reported in the last decade. These discrete effects include anticancer activity [8]. YC-1's anticancer effects seem to result from multiple action, including cell cycle arrest and apoptosis induction [9,10], anti-angiogenesis [11], anti-inflammation [12], and inhibition of matrix metalloproteinases (MMPs) [13]. Animal studies also indicate that YC-1 suppressed tumor growth and prolonged the medium survival periods in xenograft animal models carrying various human cancers (such as non-small cell lung cancer (NSCLC) [11], hepatoma [9] and prostate cancer [14]).

In this study, YC-1's cytotoxicity was examined against the Japanese Cancer Institute (JCI) human cancer cell line panel combined with database analysis to evaluate the possible application of YC-1 to cases of cancer. YC-1 exhibited middling cytotoxicity against 39 human cancer cell lines, but was more sensitive to NCI-H226 cells. We further investigated the anticancer mechanisms of YC-1 in NCI-H226 cells. Our results indicated that cell cycle arrest followed by apoptosis and the suppression of metastasis are likely to contribute to the anticancer effects of YC-1 in NCI-H226 cells. Furthermore, the possible mediating signaling pathways involved were also evaluated.

2. Materials and methods

2.1. Materials

YC-1 was synthesized and provided by one of our colleagues (Dr. Fang-Yu Lee). The purity is more than 99.0% by the examination of HPLC and NMR. In this study, YC-1 was dissolved in dimethyl sulfoxide (DMSO) to achieve the desired concentration before each experiment. The final concentration of DMSO in the culture medium was kept below 0.1%.

2.2. Human cancer cell line panel experiment

The system was developed according to the method of the National Cancer Institute [15,16], modified by the Japanese Cancer Institute [17,18]. The cancer panel experiment for YC-1 was carried out in JCI, and the inhibition profile was compared with those of more than 200 standard compounds including various anticancer drugs. The precise methods of experiments and data analysis have been described elsewhere [18]. We briefly showed the cell lines used and the method for detecting growth inhibition. The following human cancer cell lines were used in cancer panel experiments: breast cancer HBC-4, BSY-1, HBC-5, MCF-7 and MDA-MB-231; brain cancer U251, SF-268, SF-295, SF-539, SNB-75 and SNB-78; colon cancer HCC2998, KM-12, HT-29, HCT-15 and HCT-116; lung cancer NCI-H23, NCI-H226, NCI-H522, NCI-H460, A549, DMS273 and DMS114; melanoma LOX-IMVI; ovarian cancer OVCAR-3, OVCAR-4, OVCAR-5, OVCAR-8 and SK-OV-3; renal cancer RXF-631L and ACHN; stomach cancer St-4, MKN1, MKN7, MKN28, MKN45 and MKN74; and prostate cancer DU-145 and PC-3. The cell lines were cultured in RPMI-1640 (GIBCO/BRL, NY, USA) supplemented with 5% fetal bovine serum (FBS; GIBCO/BRL), penicillin (100 units/ml) (GIBCO/BRL) and streptomycin (100 μg/ml) (GIBCO/BRL) at 37 °C in humidified air containing 5% CO_2. Dose–response curves at five different concentrations between 10^{-4} and 10^{-8} M were obtained from computer analysis. The 50% growth inhibition (GI_{50}), total growth inhibition (TGI), and 50% lethal concentration (LC_{50}) values for these cell lines were determined using the sulforhodamine B (SRB) colorimetric method. Computer processing of these values produced differential activity patterns against the cell lines (mean graphs). The mean graph was compared with those of standard compounds, including various anticancer drugs, by using COMPARE analysis.

2.3. NCI-H226 cells and cell culture

Human non-small cell lung cancer cell line NCI-H226 was purchased from the American Type Culture Collection (Manassas, VA, USA). In this study, the cells were cultured in RPMI-1640 medium (GIBCO/BRL) supplemented with 10% FBS (GIBCO/BRL), 100 unit/ml penicillin/100 μg/ml streptomycin and 1% L-glutamine (GIBCO/BRL). All cells were grown in a humidified atmosphere containing 5% CO_2 at 37 °C.

2.4. Measurement of cell growth

NCI-H226 cells were seeded at 5×10^3 cells/well into 96-well plates. After 24 h incubation to allow for cell attachment, YC-1 with serial dilutions (0.1, 0.5, 0.75, 1 and 2 μM) was added to the plates, and the plates were incubated for 24, 36 and 48 h. The cell proliferation was determined by 3-(4,5-dimethylthiazol-2-yl)-2,5-diphenyltetrazolium bromide (MTT) assay. After treatment, cells were washed once with PBS and incubated with 1 mg/ml MTT (Sigma, St. Louis, MO, USA) for 2 h. Then the formazan precipitate was dissolved in 150 μl dimethyl sulfoxide and the absorbance was measured on an ELISA reader at a best wavelength of 570 nm.

2.5. Cell cycle analysis

NCI-H226 cells were seeded at 2×10^5 cells/well into 12-well plates. After 36 h incubation to allow for cell attachment, cells were treated with 2 μM YC-1 for 18, 24 and 48 h. Then both detached and attached cells were harvested and fixed with 70% ice-cold ethanol at −20 °C overnight. After fixation, cells were washed with PBS and stained with 1% Triton-X 100 (Sigma), 0.1 mg/ml RNase A (Sigma) and 4 μg/ml propidium iodide (PI, Sigma) at 37 °C for 30 min in the dark. Samples of 10,000 cells were then analyzed for DNA content by flow cytometer, using a fluorescence-activated cell sorter (FACS; Becton Dickinson, San Jose, CA, USA), and cell cycle phase distributions were analyzed by ModFit software.

2.6. Cell migration assay

Migrations of NCI-H226 cells were measured by the number of cells migrating through transwell chamber (Corning, NY,

USA). Transwell inserts with 8 μm pores were incubated with FBS-free RPMI-1640 medium for 1 h prior to the experiment. Then, cells (1×10^4 cells/100 μl FBS-free medium) were plated into the upper chambers, and 10% FBS as chemoattractant was added to the base well. After 24 h incubation to allow for cell attachment, various concentrations (0.1, 1 and 2 μM) of YC-1 in RPMI-1640 medium with 10% FBS were placed into the base well for 48 h. At the end of the experiment, cells were fixed with ice-cold methanol for 10 min and stained with Giemsa stain (Sigma) for 30 min. Cells on the upper side of the membrane were removed using a cotton swab. Then the migrated cells were counted under a light microscope at ×100 magnification.

2.7. Western blot analysis

NCI-H226 cells were seeded at 3×10^5 cells/well into 6-well culture plates. After 36 h incubation to allow for cell attachment, cells were treated with 2 μM YC-1 for 24, 36 and 48 h. Then both detached and attached cells were harvested and extracted total protein on ice with an M-PER® solution (Pierce, Rockford, IL). Total proteins (15 μg/lane) were separated on 8% SDS-PAGE (Amersham Pharmacia Biotech, Piscataway, NJ, USA) gel electrophoresis, and then transferred onto nitrocellulose membranes (Amersham Pharmacia Biotech). The membranes were blocked with 5% non-fat dry milk in TBST buffer overnight, and incubated with the desired primary antibody overnight at the following dilutions: cyclin D (1:1000), cyclin E (1:1000), CDK2 (1:1000), CDK4 (1:1000), cdc25A (1:1000), p16 (1:1000), p21 (1:1000), p53 (1:1000), Bak (1:1000), Bax (1:1000), Bcl-2 (1:1000), caspase 3 (1:1000), caspase 8 (1:1000), caspase 9 (1:1000), MMP-2 (1:400), MMP-9 (1:1000) and β-actin (1:1000). Primary antibody cyclin D, cyclin E, CDK2, CDK4, cdc25A, p16, p21, p53, Bak, Bax, Bcl-2, caspase 3, caspase 8, caspase 9, MMP-2 and MMP-9 were ordered from Upstate Biotechnology Inc., Lake Placid, NY, USA, except for β-actin (Chemicon International, Inc., Temecula, CA, USA). Subsequently, the membrane was incubated with appropriate horseradish peroxidase-conjugated secondary antibodies (Chemicon International, Inc.) for 2 h. The immunoreactive protein bands were visualized using enhanced chemiluminescence detection kit (Perkin-Elmer Life Sciences, Inc., Boston, MA, USA) and exposed to film. And then, we used the HP 3770 scanner to capture the images of protein expression and used KODAK 1D scientific image system to quantify these Western blot images.

2.8. Statistical analysis

Data are presented as the mean ± S.D. of three independent experiments. Student's *t* tests were used to assess the statistical significance of the differences, with "*p*" values of less than 0.05 being considered statistically significant.

3. Results

3.1. Human cancer cell line panel experiment

The differential activity patterns for YC-1 against 39 human cancer cell lines (mean graphs) are shown in Fig. 1. YC-1 exhibited middling cytotoxic activity, and its means for log GI_{50}, log TGI, and log LC_{50} values were −4.81, −4.39 and −4.09, respectively. However, it is more sensitive to lung cancer cell line, NCI-H226 and renal cancer cell line, RXF-631L. YC-1 was active against NCI-H226 cells, and the log GI_{50}, log TGI and log LC_{50} values were −6.65, −6.18 and −5.01. Similar effect was seen in RXF-631L cells, whereas YC-1 showed 4-fold lower log LC_{50} for NCI-H226 than that for RXF-631L. Thus the molecular mechanism by which YC-1 affects NCI-H226 cell growth was further examined in this study. The COMPARE analysis of the mean graph revealed that there is no standard anticancer drug with a high correlation coefficient to YC-1. The top one drug in their rank order of correlation coefficient is TNP-470 ($r = 0.579$).

3.2. YC-1 induced cell growth inhibition by G0/G1 phase arrest in NCI-H226 cells

Exposure to YC-1 in the concentration range of 0.1–2 μM resulted in a time- and a concentration-dependent inhibition of cell growth toward NCI-H226 cells. The IC_{50} value was approximately 0.75 μM for 48 h (Fig. 2). Then the effect of YC-1 upon cell cycle profiles was analyzed. Exposure to 2 μM YC-1 from 18 to 48 h caused an increase of G0/G1 phase population from 60.5% to 82.1%, as compared to control cells that showed 46.1% of G0/G1 phase population (Fig. 3). This result demonstrated that YC-1 induces growth-inhibitory effects via G0/G1 phase arrest. Further the G0/G1 phase-associated protein expressions were examined (Fig. 4). YC-1 induced significant increase in the expressions of p16 and p21 with a time-dependent manner. A marked increase in p53 was also observed at 24–36 h and reached the maximum activation. However, it was not detectable at 48 h. In contrast, cyclin D was gradually inhibited with a time-dependent manner, and became undetectable at 48 h. CDK4, CDK2 and cdc25A protein levels were significantly suppressed in YC-1-treated cells, which gradually decreased up to 48 h. However, the cyclin E expression level was not clearly detected in the control and YC-1-treated cells.

3.3. Long exposure to YC-1 induced apoptosis

During the cell viability assay, we observed that either high concentration of YC-1 treated or long exposure to YC-1 significantly induced cell death. Thus, we suggested that YC-1 perhaps induced apoptosis. It was verified by morphological changes (e.g., cell shrinkage and plasma membrane blebbing) and sub-G1 cells accumulated (Fig. 5A and B). The possible role of caspase was evaluated to ascertain whether or not caspase family activation participated in the apoptosis induced by YC-1 (Fig. 6A). Thirty-four kilodaltons active fragment of caspase 9 was detected at 36–48 h and then 17-kDa active fragment of caspase 3 was detected at 48 h compare with control. However, 42 kDa fragment of procaspase 8 only decreases without active fragment appearance. Further, we also found that YC-1 caused a significant increase in Bak through all treated periods, and a detectable decrease in Bcl-2 was observed at 36–48 h (Fig. 6B). However, the up-regulation of Bax protein only observed at 48 h.

3.4. YC-1 suppressed tumor cells metastasis activity in NCI-H226 cells

The cancer cells metastasis effects were investigated by cell migration assay. After being exposed to YC-1, number of cells migrated was significantly decreased less than that treated with vehicle (Fig. 7A). Then, Western blot showed that YC-1 significantly inhibited the activities of MMP-2 and MMP-9 through all treated periods (Fig. 7B).

3.5. YC-1 induced cytotoxic effect via a sGC/cGMP-independent pathway

To assess whether cGMP-dependent pathway participates in YC-1's growth-inhibitory effect, the effect of 1*H*-(1,2,4)-oxadiazolo(4,3-α)-quinoxalin-1-one (ODQ, a selective sGC inhibitor, Sigma) and KT5823 (a selective inhibitor of cGMP-dependent protein kinase, Sigma) on the YC-1-induced cytotoxic effect were examined. As shown in Fig. 8, both ODQ and KT5823 did not reverse YC-1's cytotoxic effect.

3.6. Effects of MAPK inhibitors, PD098059, SP600125 and SB203580 in YC-1-induced growth inhibition

Mitogen-activated protein kinases (MAPK) subfamilies (extracellular signal-regulated kinase (ERK), c-Jun NH_2-terminal kinase (JNK) and p38) have been reported to play crucial roles in cell death and survival [19]. ERK1/2 also has been confidently implicated in the regulation of a variety of cellular processes. To determine the role of MAPKs signaling cascades

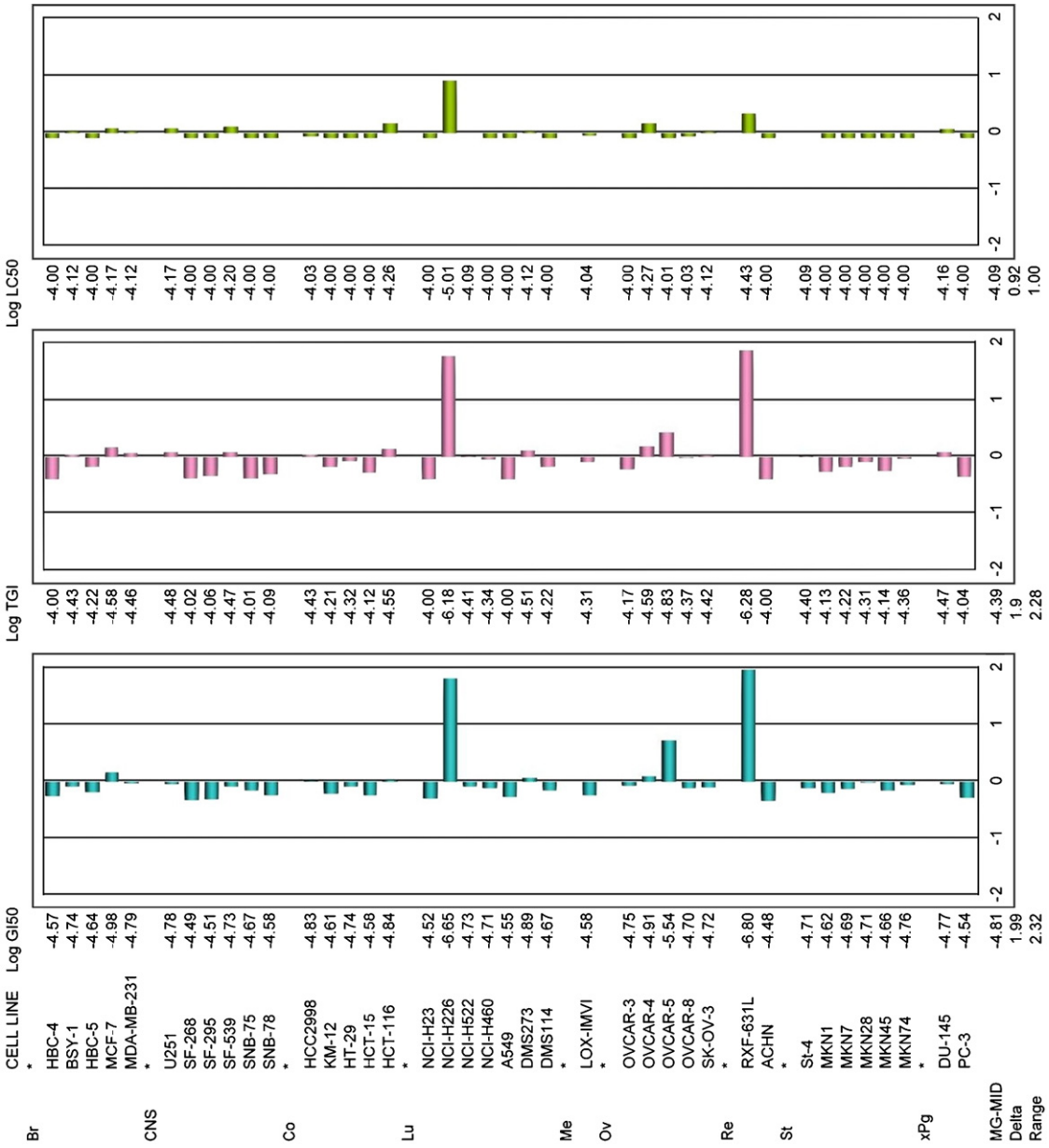

Fig. 1 – Differential activity patterns for YC-1 against 39 human cancer cell lines. MG-MID: mean of log *X* values (*X* = GI_{50}, TGI, and LC_{50}). Delta: logarithm of the difference between the MG-MID and the log *X* of the most sensitive cell line. Range: logarithm of the difference between the log *X* of the most resistant cell line and the log *X* of the most sensitive cell line.

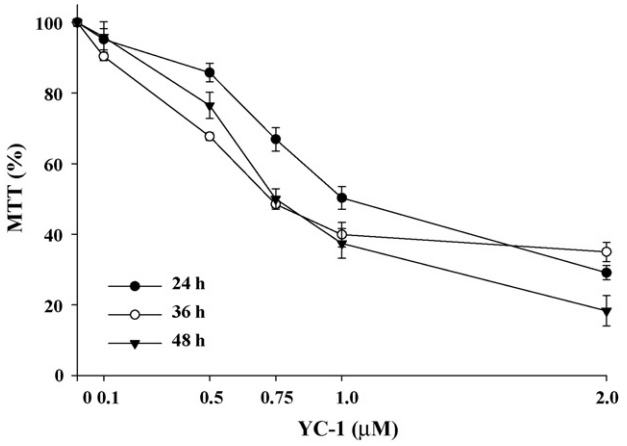

Fig. 2 – Time- and dose-dependent curves of YC-1 in MTT reduction capacity of NCI-H226 cells. Cells were treated with YC-1 at 0.1, 0.5, 0.75, 1 and 2 μM for 24, 36 and 48 h. Each value is presented as mean ± S.D. of six independent experiments.

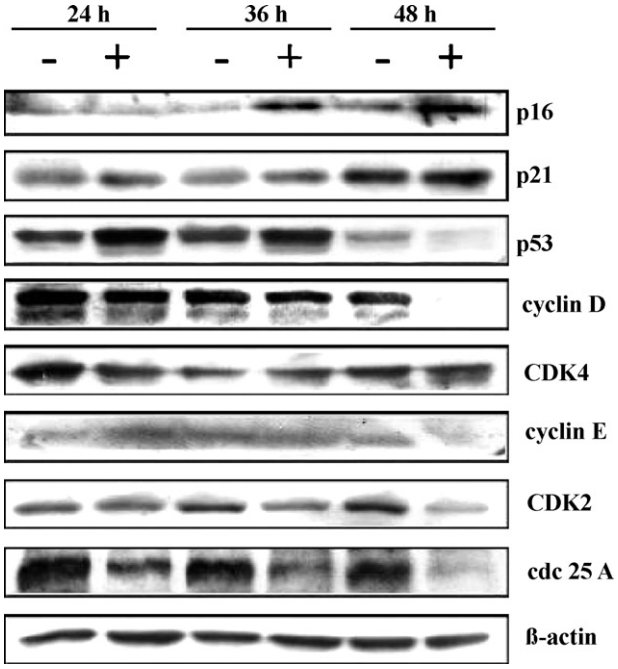

Fig. 4 – Effect of YC-1 on G0/G1 phase regulated protein expressions in NCI-H226 cells. Cells were treated with 2 μM YC-1 for 24, 36 and 48 h. Then, cells were harvested and subjected to Western blot.

for YC-1's cytotoxic effect, we have used the ERK specific inhibitors (PD98059), JNK specific inhibitor (SP600125) and p38-MAPK specific inhibitor (SB203580) on the sustained activation of MAPKs and cytotoxic effect by YC-1 were examined (Fig. 9). Cells were pretreated with or without aforementioned inhibitors for 1 h and then were stimulated with or without YC-1 for 48 h. YC-1-induced cytotoxic effects were completely and partly abolished by PD98059 and SP600125, respectively. However, SB203580 did not reverse the YC-1-induced cytotoxic effect.

4. Discussion

In previous studies, YC-1 was identified as an agent possessing versatile pharmacological actions including anticancer activity [8]. In order to search more YC-1's anticancer applications, we initially investigated this effect of YC-1 employing human cell line panel screening. The human cell line panel screening can potentially produce several results. Firstly, the panel may be used to identify compounds which possess the ability to affect the growth of human cancer cell lines. YC-1 was found to exhibit more selective inhibition on the cell growth of NCI-H226 cells. Most drugs with the same mechanism of action will show similar fingerprints against a cancer cell line database, thus the mean graph of the test compound can be matched to that of a standard anticancer drug and then the potential target or mechanism of action may be identified. The COMPARE analysis showed that YC-1 was only middling correlations with TNP-470 ($r = 0.579$). This result suggests two alternative possibilities: first, YC-1's mode of action perhaps involves that of TNP-470; second, YC-1 perhaps has a unique mode of action. In this study, we conclude that YC-1 possess multiple anticancer action mechanisms toward NCI-H226 cells, including G1 arrest of cell cycle, apoptosis and anti-metastasis.

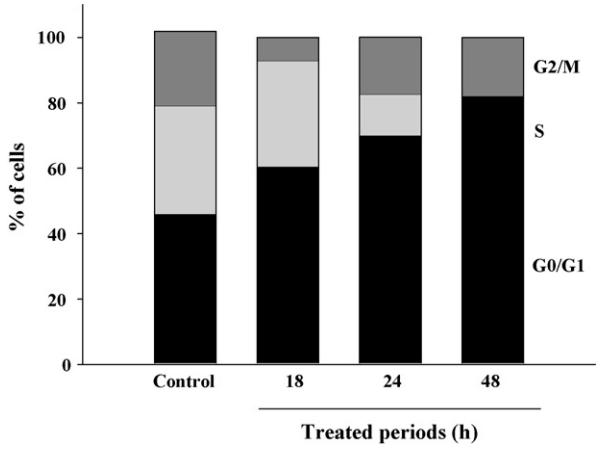

Fig. 3 – YC-1 induced G0/G1 arrest in NCI-H226 cells. Cells were treated with 2 μM YC-1 for 18, 24 and 48 h. After treatment, the cell cycle populations were examined by flow cytometry. The data is presented as mean ± S.D. from three independent experiments.

As for the mechanism by which YC-1 arrests the cell cycle, the G0/G1 phase specific regulatory protein expressions were analyzed. YC-1 caused a decrease in cyclin D, CDK4, CDK2 and cdc25A and an increase in p16, p21 and p53 to block the cell cycle at G0/G1 phase. p16 can bind and inhibit cyclin D-associated kinase (CDK4) to arrest the cell cycle at mid G1 phase, and p21 negatively regulate cyclin D/CDK2, 4 and cyclin E/CDK2 complex activity to arrest the cell cycle at late G1 phase. Further, cdc25A phosphatase is up-stream regulated protein to CDK2. Thus we demonstrated that YC-1 arrests the cell cycle at mid G1-late G1-S transition, thereby causing G1

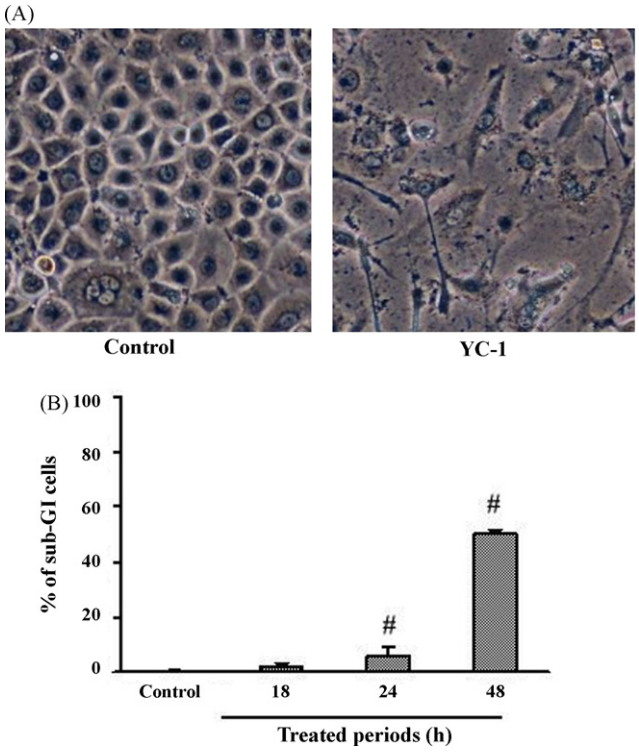

Fig. 5 – YC-1 induced apoptosis in NCI-H226 cells. (A) Morphological observation. Cells were treated with 2 μM YC-1 for 48 h, and examined using a phase contrast microscope (magnification ×200). (B) Sub-G1 cells population analysis. After treatment with 2 μM YC-1 for 18, 24 and 48 h, then the sub-G1 cells population was examined by flow cytometry. The data are presented as mean ± S.D. from four independent experiments. $^{\#}p < 0.001$ compared with control.

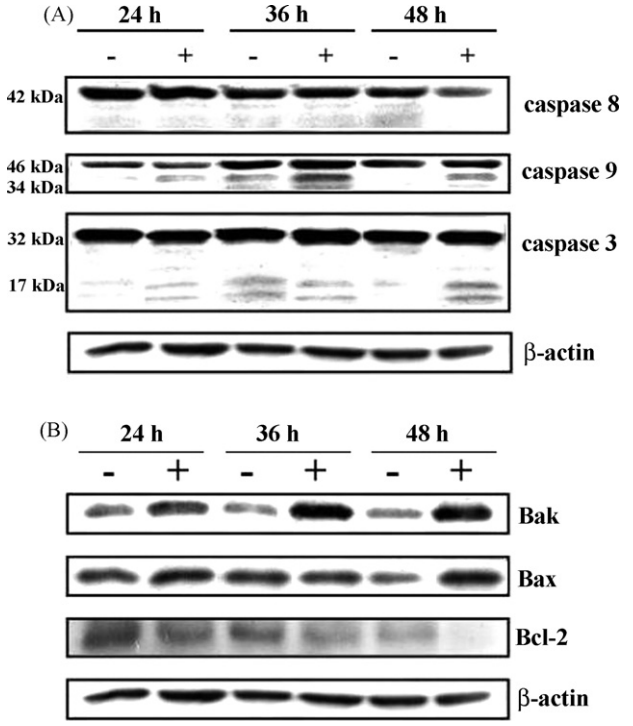

Fig. 6 – Apoptosis effects of YC-1 on the expression of apoptosis-associated proteins in NCI-H226 cells. (A) Caspase activations. (B) Bcl-2 family proteins expression. Cells were treated with 2 μM YC-1 for 24, 36 and 48 h. Then, cells were harvested and subjected to Western blot.

arrest in NCI-H226 cells. After G1 arrest, YC-1 induced apoptosis in NCI-H226 cells. YC-1 induced a cleavage of pro-caspase 9 and pro-caspase 3, but the active fragment of caspase 8 was undetectable. Caspase 3 is known to be an effector caspase, whose activation or processing triggers apoptotic cells to the ''point of no return'', whereas, caspase 9 and caspase 8 are known to be initiator caspase, which may promote apoptosis in response to mitochondria and death-inducing signals from cell surface receptors, respectively [20]. So that, YC-1-induced apoptosis might correlate with mitochondrial pathway. Further, the Bcl-2 family as the pivotal regulators of the mitochondrial pathway can either induce or inhibit the change of mitochondrial membrane potential and the release of cytochrome c into cytosol [21]. YC-1 induced an up-regulation effect in pro-apoptotic Bak and Bax. In contrast, a down-regulation effect in anti-apoptotic Bcl-2 was observed during YC-1 induced apoptosis. These results verified that YC-1-induced apoptosis indeed through mitochondrial-dependent pathway. Recent studies had evidenced that other processes in tumor progression (e.g., invasion or metastasis) perhaps are also potential targets for the development of anticancer drug [22]. Agents blocking the formation of metastasis will provide greater changes of survival for cancer patients. One family of enzymes that has been shown over the years to play a role in tumor progression is MMPs, and a number of studies have linked elevated MMP-2 and MMP-9 levels with an increased metastasis [23]. YC-1 shows significantly inhibited the MMP-9 expression and partially inhibited the MMP-2 expression, thereby suppressing the cell migration.

Elevation of the cGMP levels can be achieved by YC-1 through direct activation of sGC [5], whereas many YC-1-mediated responses went through a cGMP-independent pathway as previously described [24]. In this study, we indicated that YC-1 induced NCI-H226 cells growth-inhibitory effect by sGC/cGMP-independent signal pathway. In contrast, YC-1's growth-inhibitory effects were completely inhibited by PD98059. These results suggest that MEK/ERK pathway is involved in YC-1-induced NCI-H226 cells growth inhibition. YC-1's growth-inhibitory effect was also partially inhibited by SP600125 but was not reversed by SB20358 suggesting that the apoptosis by YC-1 was mediated through c-Jun NH_2-terminal kinase signal transduction pathway. Thus, we demonstrated that YC-1's growth-inhibitory effects are mainly mediated by extracellular signal-regulated kinase and JNK cascades, but are independent of sGC/cGMP-medicated pathway, producing alternative possible thinking that YC-1 at the dosages used for cancer chemotherapy does not produce the cGMP-mediated pharmacologic actions (e.g., increasing bleeding time and hypotension). Previously, no serious toxicity was observed in nude mice treated with YC-1 over a 2-week period [25].

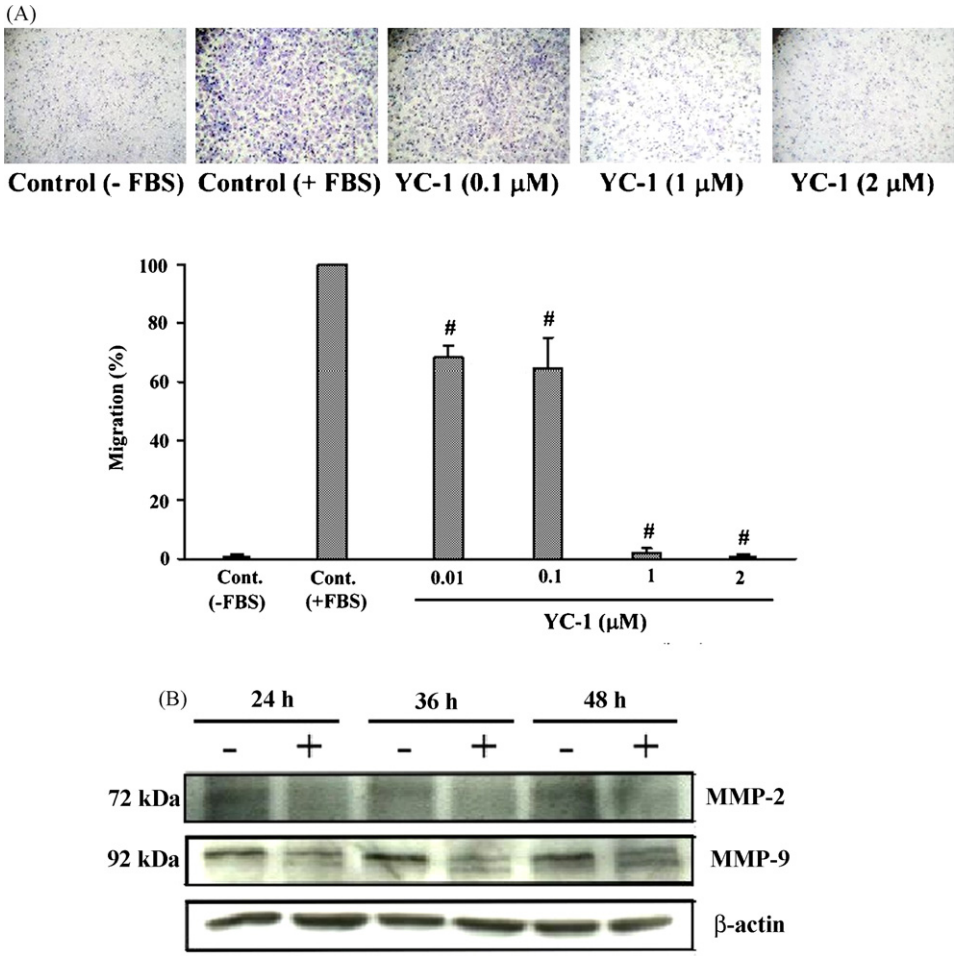

Fig. 7 – YC-1 inhibited tumor cell metastasis in NCI-H226 cells. (A) Tumor cells migration inhibition. Cells were loaded into the top chamber and treated with vehicle, 0.01, 0.1, 1 and 2 μM YC-1 for 48 h. Migrated cells were stained and counted under a light microscope. The mean ± S.D. of the relative migration rate (normalized to vehicle-treated cells as 100%) from four independent experiments is shown. $^{\#}p < 0.001$ compared with control. (B) Effect of YC-1 on MMP-2 and MMP-9 protein expressions. Cells were treated with 2 μM YC-1 for 24, 36 and 48 h. Then, cells were harvested and subjected to Western blot.

In conclusion, a clear picture of the molecular ordering of YC-1-induced events in NCI-H226 cells has emerged. YC-1 induced a decrease in cyclin D, CDK4, CDK2 and cdc25A and an increase in p16, p21 and p53 to block the cell cycle at mid G1-late G1-S transition thereby causing G1 phase arrest, coincided with Bcl-2-related proteins regulation and was followed by mitochondria-triggered caspase cascades activation and the onset of apoptosis. In addition, YC-1 also suppressed cell

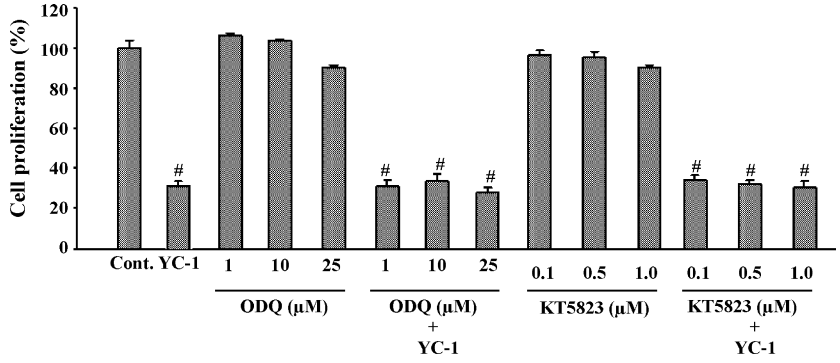

Fig. 8 – YC-1 induced cell death via a sGC/cGMP-independent pathway in NCI-H226 cells. Cells were pretreated without or with ODQ or KT5823 for 1 h, and then co-treated with YC-1 for 48 h. Effect of cell growth inhibition. The cell growth was detected by MTT assay. The data is presented as mean ± S.D. from three independent experiments. $^{\#}p < 0.001$ compared with control (with FBS).

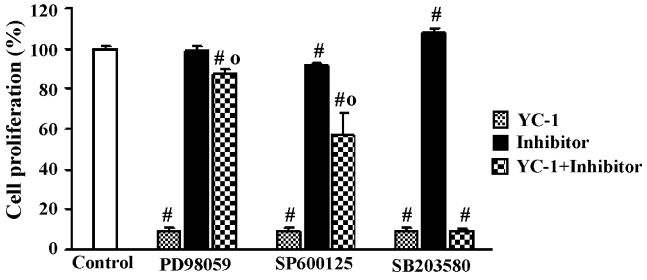

Fig. 9 – YC-1 induced cell death by the JNK and ERK cascades in NCI-H226 cells. Cells were pretreated without or with inhibitors (PD98059, SP600125 or SB203580) for 1 h, and then co-treated with 2 μM YC-1 for 48 h. The concentrations of PD98059, SP600125 and SB203580 are 10, 15 and 10 μM, respectively. The data is presented as mean ± S.D. from three independent experiments. $^{\#}p < 0.001$ compared with control. $^{\circ}p < 0.001$ compared with YC-1 used alone.

migration via down-regulating of MMP-2 and MMP-9 activities. These series of events confirmed above human cell line panel screening results producing one possibility, indicating that YC-1's mode of action involves that of TNP-470. Many reports previously indicated that TNP-470 possess anticancer activity medicating by G0/G1 arrest [26], NO-enhancing to induce apoptosis, and cell migration inhibiting [27]. But TNP-470 produced neurotoxicity at dose where anticancer activity was seen in clinical trial [28]. Thus YC-1 is more worth investigating further in terms of its clinical applications in cancer therapy.

Acknowledgement

This work was supported by a research grant from the National Science Council (NSC95-2323-B039-001) in Taiwan awarded to S.C. Kuo.

REFERENCES

[1] Jemal A, Siegel R, Ward E, Murray T, Xu J, Smigal C, et al. Cancer statistics, 2006. CA Cancer J Clin 2005;55:106–30.
[2] Department of Health. Vital Statistics, 2004. Taipei: Department of Health; 2005.
[3] Sawyers C. Targeted cancer therapy. Nature 2004;432:294–7.
[4] Ko FN, Wu CC, Kuo SC, Lee FY, Teng CM. YC-1, a novel activator of platelet guanylate cyclase. Blood 1994;84: 4226–33.
[5] Wu CC, Ko FN, Kuo SC, Lee FY, Teng CM. YC-1 inhibited human platelet aggregation through NO-independent activation of soluble guanylate cyclase. Br J Pharmacol 1995;116:1973–8.
[6] Teng CM, Wu CC, Ko FN, Lee FY, Kuo SC. YC-1, a nitric oxide-independent activator of soluble guanylate cyclase, inhibits platelet-rich thrombosis in mice. Eur J Pharmacol 1997;320:161–6.
[7] Friebe A, Schultz G, Koesling D. Stimulation of soluble guanylate cyclase by superoxide dismutase is mediated by NO. Biochem J 1998;335:527–31.
[8] Chun YS, Yeo EJ, Park JW. Versatile pharmacological actions of YC-1: anti-platelet to anticancer. Cancer Lett 2004;207:1–7.
[9] Wang SW, Pan SL, Guh JH, Chen HL, Huang DM, Chang YL, et al. YC-1 [3-(5′-Hydroxymethyl-2′-furyl)-1-benzyl Indazole] exhibits a novel antiproliferative effect and arrests the cell cycle in G0-G1 in human hepatocellular carcinoma cells. J Pharmacol Exp Ther 2005;312: 917–25.
[10] Yeo EJ, Ryu JH, Chun YS, Cho YS, Jang IJ, Cho H, et al. YC-1 induces S cell cycle arrest and apoptosis by activating checkpoint kinases. Cancer Res 2006;66:6345–52.
[11] Pan SL, Guh JH, Peng CY, Wang SW, Chang YL, Cheng FC, et al. YC-1 [3-(5′-hydroxymethyl-2′-furyl)-1-benzyl indazole] inhibits endothelial cell functions induced by angiogenic factors in vitro and angiogenesis in vivo models. J Pharmacol Exp Ther 2005;314: 35–42.
[12] Pan SL, Guh JH, Peng CY, Chang YL, Cheng FC, Chang JH, et al. A potential role of YC-1 on the inhibition of cytokine release in peripheral blood mononuclear leukocytes and endotoxemic mouse models. Thromb Haemost 2005;93:940–8.
[13] Liu YN, Pan SL, Peng CY, Guh JH, Huang DM, Chang YL, et al. YC-1 [3-(5′-hydroxymethyl-2′-furyl)-1-benzyl indazole] inhibits neointima formation in balloon-injured rat carotid through suppression of expressions and activities of matrix metal-oproteinases 2 and 9. J Pharmacol Exp Ther 2006;316:35–41.
[14] Huang YT, Pan SL, Guh JH, Chang YL, Lee FY, Kuo SC, et al. YC-1 suppresses constitutive nuclear factor-kappaB activation and induces apoptosis in human prostate cancer cells. Mol Cancer Ther 2005;4:1628–35.
[15] Paull KD, Shoemaker RH, Hodes L, Monks A, Scudiero DA, Rubinstein L, et al. Display and analysis of patterns of differential activity of drugs against human tumor cell lines: development of mean graph and COMPARE algorithm. J Natl Cancer Inst 1989;81:1088–92.
[16] Monks A, Scudiero D, Skehan P, Shoemaker R, Paull K, Vistica D, et al. Feasibility of a high-flux anticancer drug screen using a diverse panel of cultured human tumor cell lines. J Natl Cancer Inst 1991;83:757–66.
[17] Yamori T, Matsunaga A, Sato S, Yamazaki K, Komi A, Ishizu K, et al. Potent antitumor activity of MS-247, a novel DNA minor groove binder, evaluated by an in vitro and in vivo human cancer cell line panel. Cancer Res 1999;59:4042–9.
[18] Yamori T. Panel of human cancer cell lines provides valuable database for drug discovery and bioinformatics. Cancer Chemother Pharmacol 2003;52(1):S74–9.
[19] English J, Pearson G, Wilsbacher J, Swantek J, Karandikar M, Xu S, et al. New insights into the control of MAP kinase pathways. Exp Cell Res 1999;253:255–70.
[20] Herr I, Debatin KM. Cellular stress response and apoptosis in cancer therapy. Blood 2001;98:2603–14.
[21] Ruvolo PP, Deng X, May WS. Phosphorylation of Bcl-2 and regulation of apoptosis. Leukemia 2001;15:515–22.
[22] Rosen L. Antiangiogenic strategies and agents in clinical trials. Oncologist 2000;5:20–7.
[23] John A, Tuszynski G. The role of matrix metalloproteinases in tumor angiogenesis and tumor metastasis. Pathol Oncol Res 2001;7:14–23.
[24] Ferrero R, Torres M. Prolonged exposure to YC-1 induces apoptosis in adreno-medullary endothelial and chromaffin cells through a cGMP-independent mechanism. Neuropharmacology 2001;41:895–906.
[25] Yeo EJ, Chun YS, Cho YS, Kim J, Lee JC, Kim MS, et al. YC-1: a potential anticancer drug targeting hypoxia-inducible factor 1. J Natl Cancer Inst 2003;95:516–25.

[26] Zhang Y, Griffith EC, Sage J, Jacks T, Liu JO. Cell cycle inhibition by the anti-angiogenic agent TNP-470 is mediated by p53 and p21WAF1/CIP1. Proc Natl Acad Sci USA 2000;97:6427–32.
[27] Yoshida T, Kaneko Y, Tsukamoto A, Han K, Ichinose M, Kimura S. Suppression of hepatoma growth and angiogenesis by a fumagillin derivative TNP470: possible involvement of nitric oxide synthase. Cancer Res 1998;58:3751–6.
[28] Bhargava P, Marshall JL, Rizvi N, Dahut W, Yoe J, Figuera M, et al. A Phase I and pharmacokinetic study of TNP-470 administered weekly to patients with advanced cancer. Clin Cancer Res 1999;5:1989–95.